JOM, Vol. 66, No. 12, 2014
DOI: 10.1007/s11837-014-1181-y
© 2014 The Minerals, Metals & Materials Society

Improved High-Temperature Microstructural Stability and Creep Property of Novel Co-Base Single-Crystal Alloys Containing Ta and Ti

F. XUE,[1] H.J. ZHOU,[2] and Q. FENG[1,2,3]

1.—State Key Laboratory for Advanced Metals and Materials, University of Science and Technology Beijing, Beijing 100083, China. 2.—National Center for Materials Service Safety, University of Science and Technology Beijing, Beijing 100083, China. 3.—e-mail: qfeng@skl.ustb.edu.cn

The influence of Ta and Ti additions on microstructural stability and creep behavior in novel Co-Al-W base single-crystal alloys has been investigated. Compared to the ternary alloy, the γ' solvus temperature and γ' volume fraction were raised by individual additions of Ta and Ti, and increased further in the quinary alloy containing both alloying additions. In contrast to ternary and quaternary alloys, an improved microstructural stability with the stable γ–γ' two-phase microstructure and more than 60% γ' volume fraction existed in the quinary alloy after prolonged aging treatment at 1050°C for 1000 h. The creep behavior at 900°C revealed lower creep rates and longer rupture lives in the quaternary alloys compared to the ternary alloy, whereas the quinary alloy exhibited even better creep resistance. When the creep temperature was elevated to about 1000°C, the creep resistance of the quinary alloy exceeded the previously reported Co-Al-W-base alloys and first-generation Ni-base single-crystal superalloys. The improved creep resistance at approximately 1000°C was considered to be associated with high γ' volume fraction, γ' directional coarsening, and dislocation substructure, which included γ–γ' interfacial dislocation networks and the sheared γ' precipitates containing stacking faults and anti-phase boundaries.

INTRODUCTION

Nickel-base superalloys have been used in gas turbine applications for decades because of their superior high-temperature mechanical properties strengthened by $L1_2$-type γ' precipitates.[1,2] The recently reported Co-Al-W-base alloys exhibited similar γ–γ' two-phase microstructure and anomalous increase of flow strength at elevated temperature,[3,4] and their single crystal alloys were comparable to first-generation Ni-base single-crystal superalloys in creep resistance at 900°C.[5–7] These investigations indicated that this class of novel Co-base alloys was promising structural materials for high-temperature applications.

In an attempt to increase the γ' solvus temperature that was highly responsible for the high-temperature strength in γ–γ' two-phase alloys, various alloying additions have been investigated in Co-Al-W-base alloys.[4,8–12] The γ' solvus temperature was significantly raised in their quaternary alloys by individual additions of Ta, Ti, Nb, and V, whereas a few of them exceeded 1100°C. Furthermore, the microstructural instability by the formation of secondary phases with a high level of refractory alloying elements frequently occurred because of the very narrow region of γ–γ' two phase.[4,5,8,9]

The investigations on high-temperature mechanical properties are relatively limited in Co-Al-W-base alloys, especially for the creep properties of single-crystal alloys.[4–6,13,14] Creep research revealed a pronounced increase of high-temperature strength by Ta and Ti additions in quaternary alloys, which was expected to be associated with high γ' solvus temperature and microstructural stability. However, these investigations have been focused mainly on ternary and quaternary alloys within a

 (Published online October 15, 2014)

Table I. Nominal compositions in at.% and γ' solvus temperatures of Co-Al-W base alloys

Group	Alloy	Co	Al	W	Ta	Ti	Ta+Ti	γ' solvus temperature (°C)
I	Base alloy	Bal.	7	8	–	–	0	919
	Alloy Ta	Bal.	7	8	1	–	1	998
	Alloy Ti	Bal.	7	8	–	4	4	1070
	Alloy TaTi	Bal.	7	8	1	4	5	1131[16]
II	Alloy TaTi-A	Bal.	8.6	6.6	1.7	2	3.7	1097
	Alloy TaTi-B	Bal.	7	8	1	4	5	1131
	Alloy TaTi-C	Bal.	7	7	2	4	6	1157[16]
	Alloy TaTi-D	Bal.	6	6	2	6	8	1184
	Alloy TaTi-E	Bal.	6.3	4.4	3	4	7	1146

narrow temperature range from 850°C to 950°C because of a relatively limited γ' volume fraction at a higher temperature. Few attempts have been made to illustrate a fundamental creep deformation mechanism.[5,6,13,14] Additionally, different rafting behavior from commercial Ni-base single-crystal superalloys was observed in Co-base alloys with positive misfit,[5,6,15] but its role in creep behavior and strengthening was still not clear, in particular at temperatures above 950°C.

In our previous research, Co-Al-W-Ta-Ti quinary alloys with higher γ' solvus temperature and better microstructural stability than quaternary alloys containing Ta or Ti additions were designed based on fundamental studies on ternary and quaternary alloys.[9,15–18] This investigation aims at understanding the individual and synergetic effects of Ta and Ti additions on γ' thermal stability, microstructural stability, and high-temperature creep behavior in single-crystal alloys. Of special interest are their influence on γ' solvus temperature, γ–γ' two-phase microstructural evolution during long-term aging, phase equilibrium, creep behavior, and deformation mechanism at approximately 1000°C under different levels of applied stress.

EXPERIMENTAL PROCEDURES

The nominal compositions and abbreviated names of the experimental alloys are listed in Table I. The experimental alloys, divided by Groups I and II, were designed to compare the individual and synergetic effects of Ta and Ti additions. Note alloy TaTi in Group I has the same composition as alloy TaTi-B in Group II. Group I single-crystal bars were directionally solidified using the Bridgman method with 15 mm in diameter and 150 mm in length. All the Groups I and II alloys were solution heat treated at 1250–1270°C for 24 h before aging at 900–1100°C for various times followed by air cooling. The Group I specimens within 10° away from [001] direction were aged at 900°C for 50 h before being crept in air at 900°C/420 MPa. Creep tests at 1000°C/137 MPa and 982°C/248 MPa were specially conducted for alloy TaTi because of its better microstructural stability. Two stress levels were employed to understand deformation modes during creep and for a direct comparison with previously reported results for Co-base and Ni-base single-crystal alloys. The γ' solvus temperatures of Group I and Group II alloys were measured based on the differential scanning calorimetry (DSC) heating curves with a heating rate of 10°C/min. The γ' sizes were determined as the spherical equivalent diameters by using the Image-Pro software (MediaCybernetics Inc., Rockville, MD) through at least three scanning electron microscopy images. The details of microstructure characterization, microstructure analysis, and sample preparation, such as optical microscopy, scanning electron microscopy, and transmission electron microscopy, have been reported elsewhere.[9,15,16]

RESULTS

γ' Solvus Temperature

The γ' solvus temperatures of Group I and Group II alloys, determined by DSC, are shown in Table I. In Group I, the Ta and Ti additions in quaternary and quinary alloys led to all the γ' solvus temperatures rising by approximately 80–240°C compared with the ternary alloy. Alloy Ti containing 4 at.% Ti exhibited γ' solvus temperature 72°C higher than alloy Ta with 1 at.% Ta addition, and it was further increased by 61°C in alloy TaTi because of their combined additions. All Groups I and II quinary alloys containing both Ta and Ti additions possessed much higher γ' solvus temperatures than the ternary and quaternary alloys. Although there were some variations in the Al and W concentrations, the general trend showed that these temperatures increased with increasing the total content of Ta and Ti. For example, the γ' solvus temperature of alloy TaTi-A containing 1.7 at.% Ta and 2 at.% Ti was 1097°C, and it steadily increased to 1157°C in alloy TaTi-C as the sum content of Ta and Ti additions reached 6 at.%. It should be noted that a relatively lower γ' solvus temperature of 1146°C occurred in alloy TaTi-E containing 7 at.% (Ta+Ti), mainly because of the less W content.

Microstructural Stability

The short-term aging treatment was first used to assess the formation of γ–γ' two-phase microstructure. This aging produced different amounts of χ

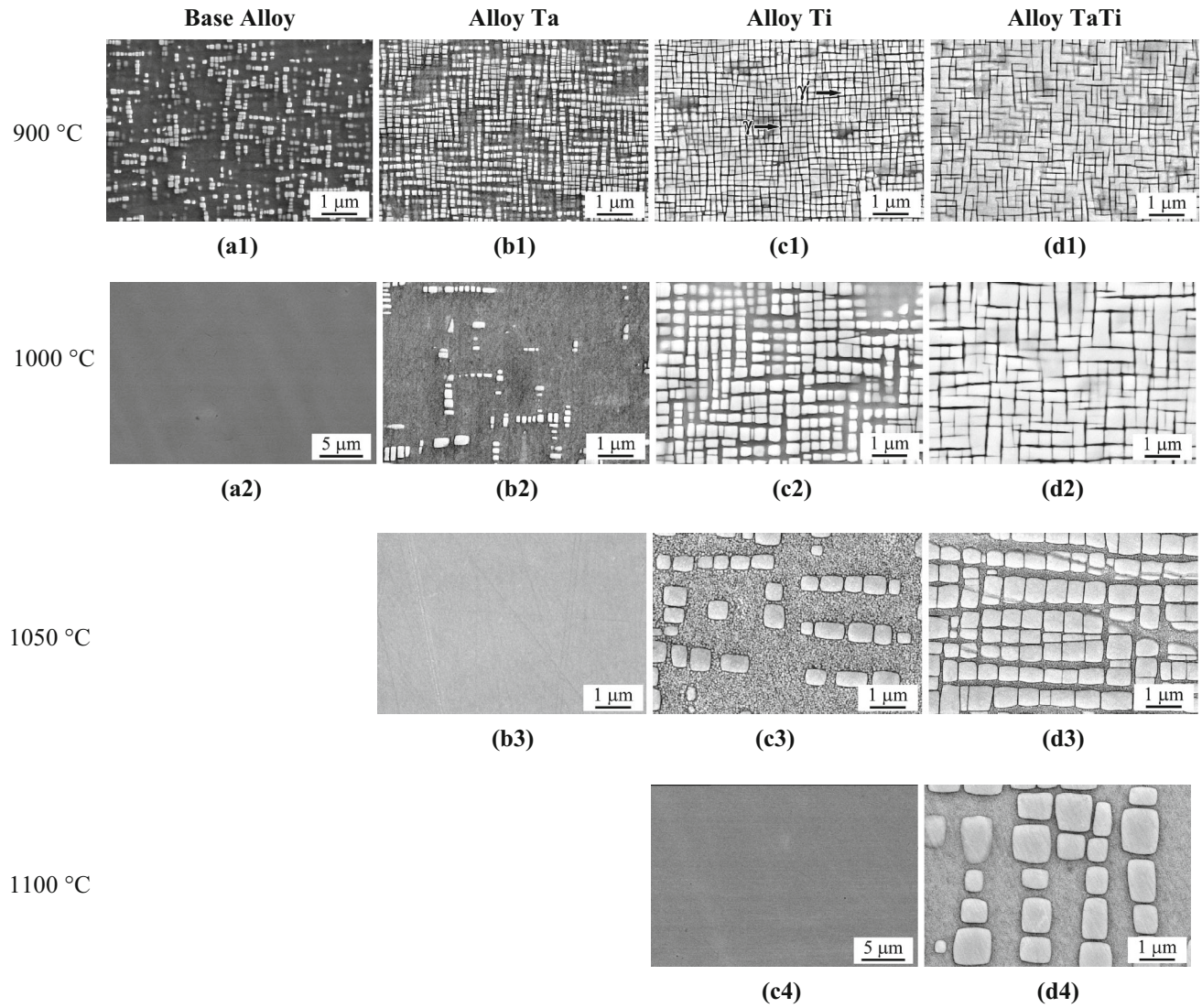

Fig. 1. Typical microstructure of solutioned Group I alloys after aging at 900–1100°C for 50 h: (a1–d1) 900°C, (a2–d2) 1000°C, (b3–d3) 1050°C, and (c4–d4) 1100°C.

and/or β phases in many quinary alloys in Group II; therefore, only the alloys in Group I were compared to isolate the effects of Ta and Ti additions on γ' stability and creep behavior. Figure 1 shows the typical microstructure of Group I alloys after aging at 900–1100°C for 50 h. These alloys either exhibited γ single-phase or γ–γ' microstructure without the presence of secondary phases. At 900°C (Fig. 1a1–d1), the γ' volume fraction gradually increased from 15.3% to 87.6% as the levels of Ta+Ti content increased. This tendency was also present at the higher aging temperatures. Figure 1a2, b3, and c4 illustrate that base alloy, alloy Ta, and alloy Ti were γ single phase at 1000°C, 1050°C, and 1100°C, respectively, which is in good agreement with the measured γ' solvus temperature trends for these alloys (Table I). It is indicated that the thermal stability of γ' phase was more strongly promoted by 4 at.% Ti addition than 1 at.% Ta addition, and their combination resulted in the alloy with the most stable γ' phase at a high temperature.

Long-term aging at 900°C was carried out to evaluate alloying effects on microstructural stability. Figure 2 exhibits the typical microstructure of Group I alloys after prolonged aging at 900°C for 600–2000 h. The γ' precipitates almost disappeared in the base alloy after aging for 600 h (Fig. 2a). In addition to γ–γ' phases, an appropriate amount of plate-like χ precipitates (Co-1.6Al-17.7W-4.9Ta, at.%) with preferential orientation were observed in alloy Ta after aging for 2000 h (Fig. 2b), whereas no secondary phases were evident in alloy Ti and alloy TaTi (Fig. 2c and d). Although the γ' volume fractions slightly decreased after long-term aging at 900°C, they were still as high as 70.1% and 81.2% in alloy Ti and alloy TaTi, respectively.

Long-term microstructural stability was further investigated in alloy TaTi at temperatures above

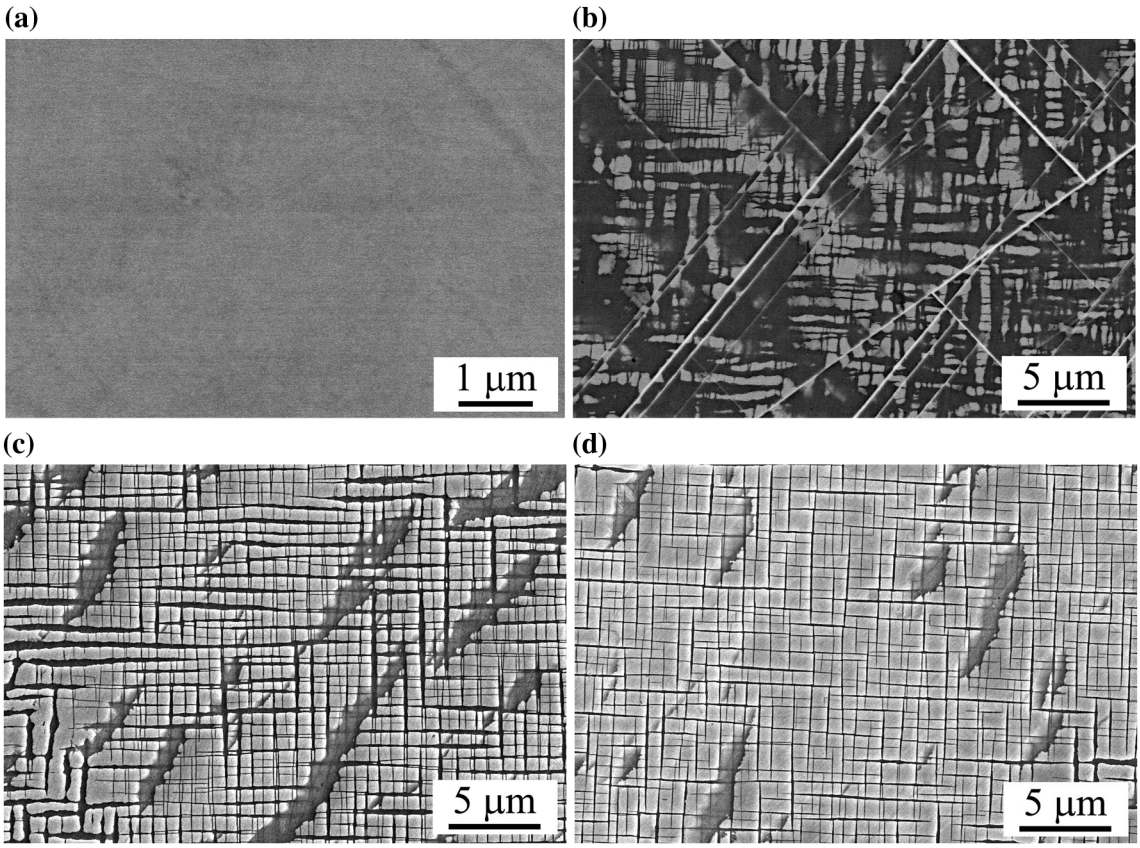

Fig. 2. Typical microstructure of solutioned Group I alloys after long-term aging at 900°C: (a) base alloy, 600 h; (b) alloy Ta, 2000 h; (c) alloy Ti, 2000 h; and (d) alloy TaTi, 2000 h.

1000°C. As shown in Fig. 3, the γ–γ' two-phase microstructure remained and no secondary phases were observed after aging at 1000°C and 1050°C for 1000 h. The γ' precipitates exhibited cuboidal morphology, and their γ' volume fractions were 75.0% at 1000°C and 63.8% at 1050°C. It is clear that the combined Ta and Ti additions in the quinary alloy stabilizes the γ' phase at these elevated temperatures unlike the ternary and quaternary alloys.

Creep Behavior

The initial γ' volume fraction and γ' size of Group I alloys aged at 900°C for 50 h before creep testing are listed in Table II. Figure 4a–c and Table III show the creep curves and creep properties of Group I alloys at 900°C/420 MPa, 1000°C/137 MPa, and 982°C/248 MPa, respectively. At 900°C, the creep rupture life of the base alloy was less than 3 min, whereas they increased to 24.0 h and 59.3 h by 1 at.% Ta and 4 at.% Ti additions, respectively, and significantly prolonged to 201.2 h in alloy TaTi (Fig. 4a). Although Ti addition was more effective than Ta addition in lowering the creep rate in comparison with the ternary alloy, the quinary alloy possessed the lowest creep rate and the strongest creep resistance as shown in Table III. With increasing the temperature, alloy TaTi presented a creep life of 475.2 h with 1% plastic strain at 1000°C/137 MPa, which exceeds the previously reported creep rupture life of Co-base alloys under the same testing condition (included in Fig. 4b and Table III).[6] With increasing the high stress level, alloy TaTi had a creep rupture life of 122.0 h that fell in between the first- and second-generation Ni-base single-crystal superalloys CMSX-3 (90.1 h) and CMSX-4 (178.0 h), as shown in Fig. 4c and Table III.[19]

Post-Crept Microstructure

Figure 5 shows the typical microstructure in the longitudinal Sections 5 mm away from the fracture surface of Group I alloys after creep rupture at 900°C/420 MPa. With increasing γ' volume fraction in quaternary and quinary alloys, large-sized γ' rafts or rods were observed due to directional coarsening during creep (Fig. 5b–d). These γ' rafts were parallel to the tensile stress axis, indicative of a positive γ–γ' misfit at this temperature. Additional plate-like χ precipitates existed near the fracture surface of alloy Ta and appeared to promote crack propagation.

The postcrept microstructure and dislocation configurations of alloy TaTi alloys were examined in an attempt to illustrate the deformation mecha-

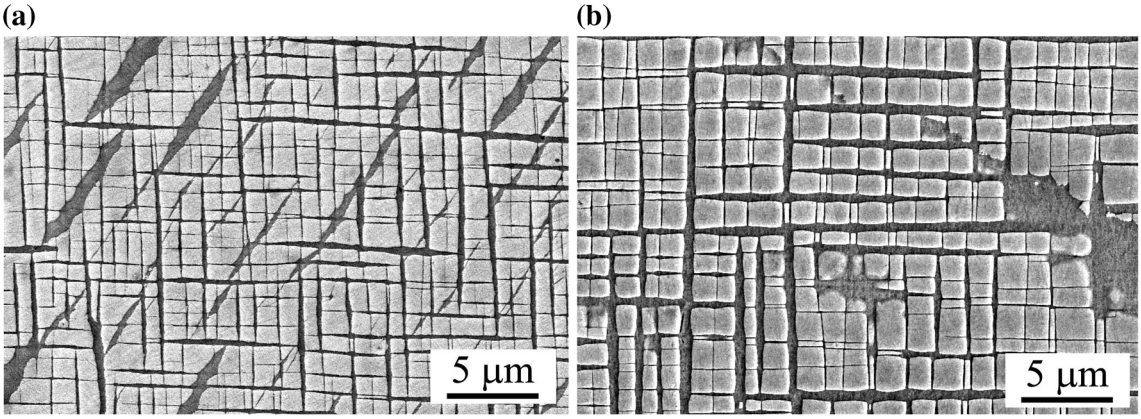

Fig. 3. Typical microstructure of solutioned alloy TaTi after long-term aging: (a) 1000°C, 1000 h; and (b) 1050°C, 1000 h.

Table II. γ' volume fraction and γ' size of Group I alloys aged at 900°C for 50 h before creep test

Alloy	γ' volume fraction (%)	γ' size (μm)
Base alloy	15.3 ± 1.8	0.10 ± 0.02
Alloy Ta	33.4 ± 2.8	0.12 ± 0.03
Alloy Ti	74.5 ± 1.3	0.16 ± 0.04
Alloy TaTi	87.6 ± 1.8	0.21 ± 0.06

nisms at approximately 1000°C after 1% creep strain after the tertiary creep stage began. Figure 6a shows the typical three-dimensional microstructures of alloy TaTi under 137 MPa for 475.2 h. The directionally coarsened γ' precipitates parallel to the applied tensile stress were well defined on the (100) and (010) planes. These rafts were consistent with the regular interpenetrating lamellar structure on the horizontal section perpendicular to loading direction. For a higher stress level (248 MPa), the γ' rafts with similar morphology developed, although they were noticeably smaller in size, probably because of the short creep time (26.1 h) after 1% creep strain at 982°C, as illustrated in Fig. 6b.

The general defects after 1% creep stain at 1000°C were identified using transmission electron microscopy. The identified substructures included γ–γ' interfacial dislocation networks and dislocations coupled with stacking faults (SFs) and antiphase boundaries (APBs) within γ' precipitates. Figure 7a shows the typical dislocation networks at the γ–γ' interfaces, which appeared to exist preferentially in the parallel to load section rather than the perpendicular to load section in alloy TaTi. A high density of dislocations with SFs was evident in a single raft and frequently intersected each other (Fig. 7a), implying the occurrence of sheared γ' precipitates by activating multiple ⟨112⟩ slips. APBs were also observed in γ' precipitates and often coexisted with SFs as marked by arrows in Fig. 7b; these APBs indicate a variation from shearing by ⟨112⟩ slip with an intermediate step, e.g., the entire 1/2⟨110⟩ dislocations entered into the precipitates and left APBs in their lake which were then removed by the Shockley loops.[20] For alloy TaTi after 1% creep strain under high stress level (248 MPa), although similar dislocation substructures with SFs and APBs were present within γ' precipitates, the interfacial dislocation spacings in networks were wide as shown in Fig. 7c.

DISCUSSION

γ' Thermal Stability and Microstructural Stability

The γ' thermal stability is essential for improving γ' strengthening and temperature capability in most advanced Ni-base superalloys.[1] Previous investigations showed that Ta, Ti, Nb, and V were γ' forming elements and raised the γ' solvus temperatures of Co-Al-W-base alloys to different extents, among which Ta addition always possessed the most significant influence.[4,8–10] In the current study, the increase of γ' solvus temperature by individual additions of Ta and Ti was consistent with previous experimental results, whereas the more effective influence of Ti addition appeared because of its higher content (4 at.%) than Ta addition (1 at.%). The further increased amounts of γ'-forming elements were expected to promote the γ' solvus temperature continuously in all quinary alloys (Table I), whereas it is indicated that the interaction between them also provided a significant contribution.

The γ–γ' two-phase region is in a very narrow composition range of the Co-Al-W ternary system. With Ta addition, the γ–γ' two-phase region remains narrow at 900°C,[3,21] however, it expands when adding Ti.[22] For aging at 900°C for 2000 h, the current study shows that the composition of base alloy is in the γ single-phase region, whereas the χ phase coexisted with γ–γ' microstructure for alloy Ta and more than 70% γ' volume fraction remained without secondary phases in alloy Ti. Thus, for 900°C phase equilibria, the ternary alloy remains in

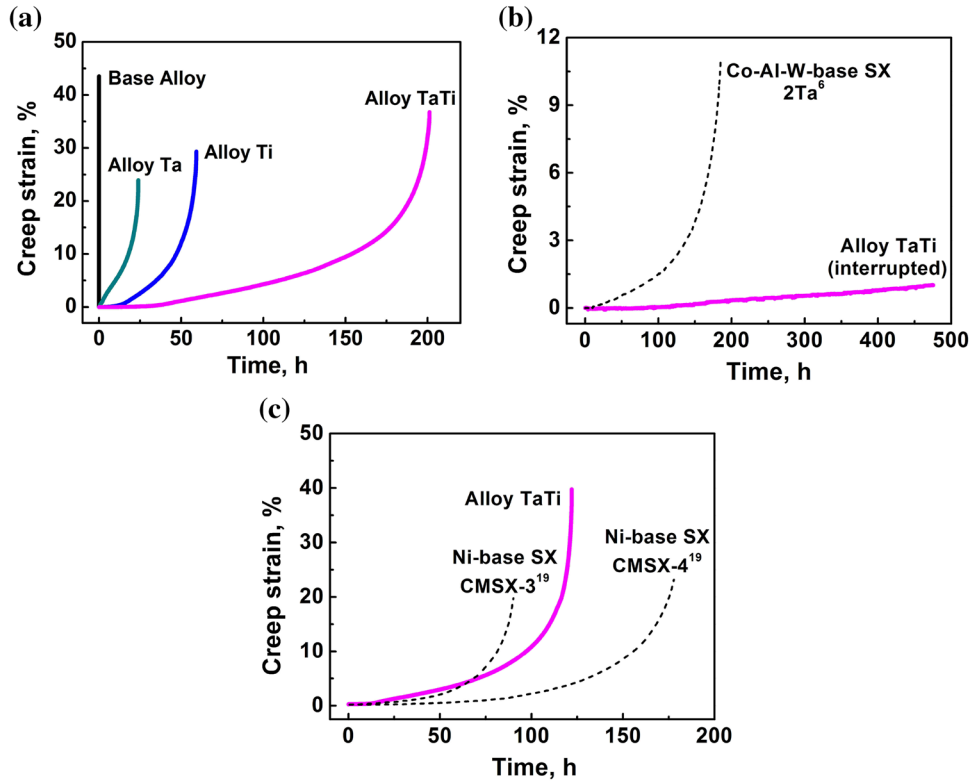

Fig. 4. Comparison of tensile creep curves of Group I alloys with previously reported Co-Al-W-base and Ni-base single-crystal alloys:[6,19] (a) 900°C/420 MPa, (b) 1000°C/137 MPa, and (c) 982°C/248 MPa.

Table III. Creep properties of Group I alloys, Co-base alloy Co-9Al-10W-2Ta, and Ni-base single-crystal superalloys CMSX-3 and CMSX-4 at 900°C to 1000°C[6,19]

Condition	Alloy	Rupture time (h)	Elongation (%)
900°C	Base alloy	0.05	43.2
248 MPa	Alloy Ta	24.0	23.3
	Alloy Ti	59.3	37.5
	Alloy TaTi	201.2	36.7
1000°C	Alloy TaTi	475.2 (interrupted)	1.0 (interrupted)
137 MPa	Co-9Al-10W-2Ta[6]	187.9	14.3
982°C	Alloy TaTi	122.0	39.5
248 MPa	CMSX-3[19]	90.1	24.5
	CMSX-4[19]	178.0	26.8

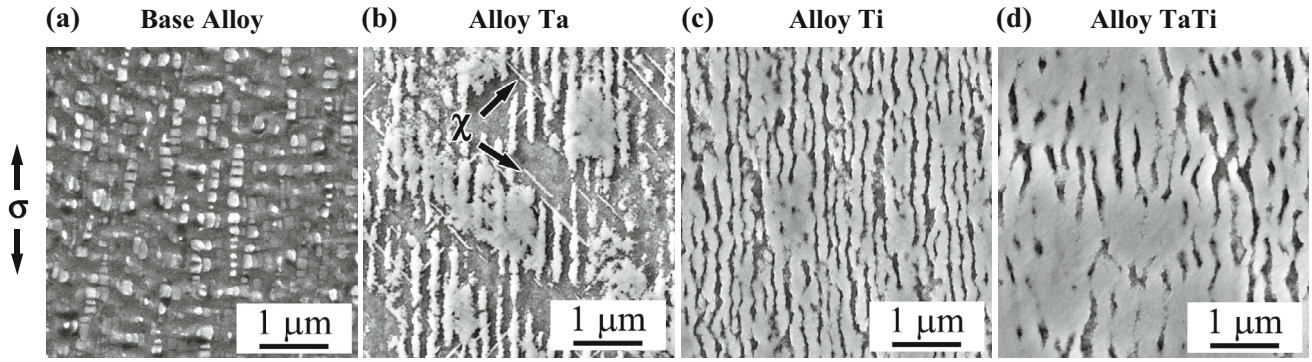

Fig. 5. Typical microstructure of longitudinal sections of Group I alloys after creep rupture at 900°C/420 MPa. Note that the observations were 5 mm away from the fracture surface.

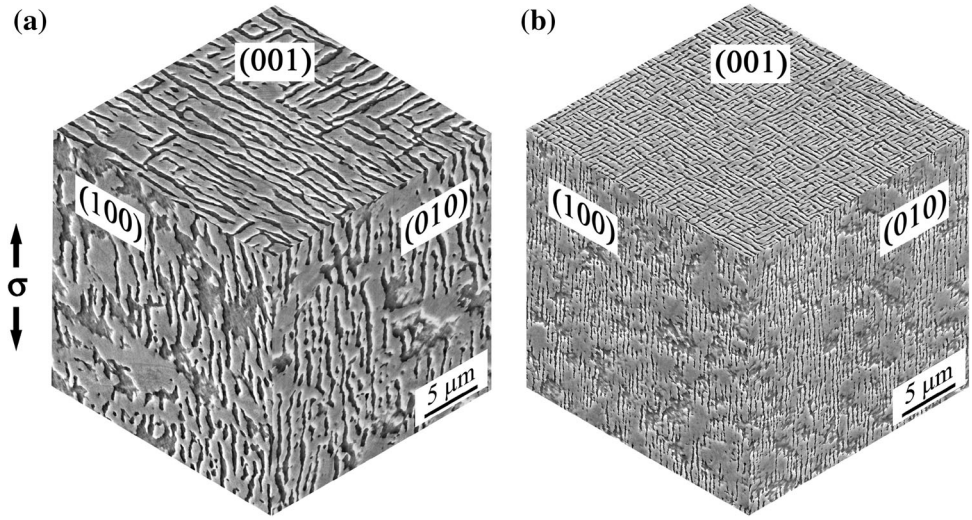

Fig. 6. Three-dimensional microstructures of alloy TaTi after 1% creep strain: (a) 1000°C/137 MPa, 475.2 h, and (b) 982°C/248 MPa, 26.1 h.

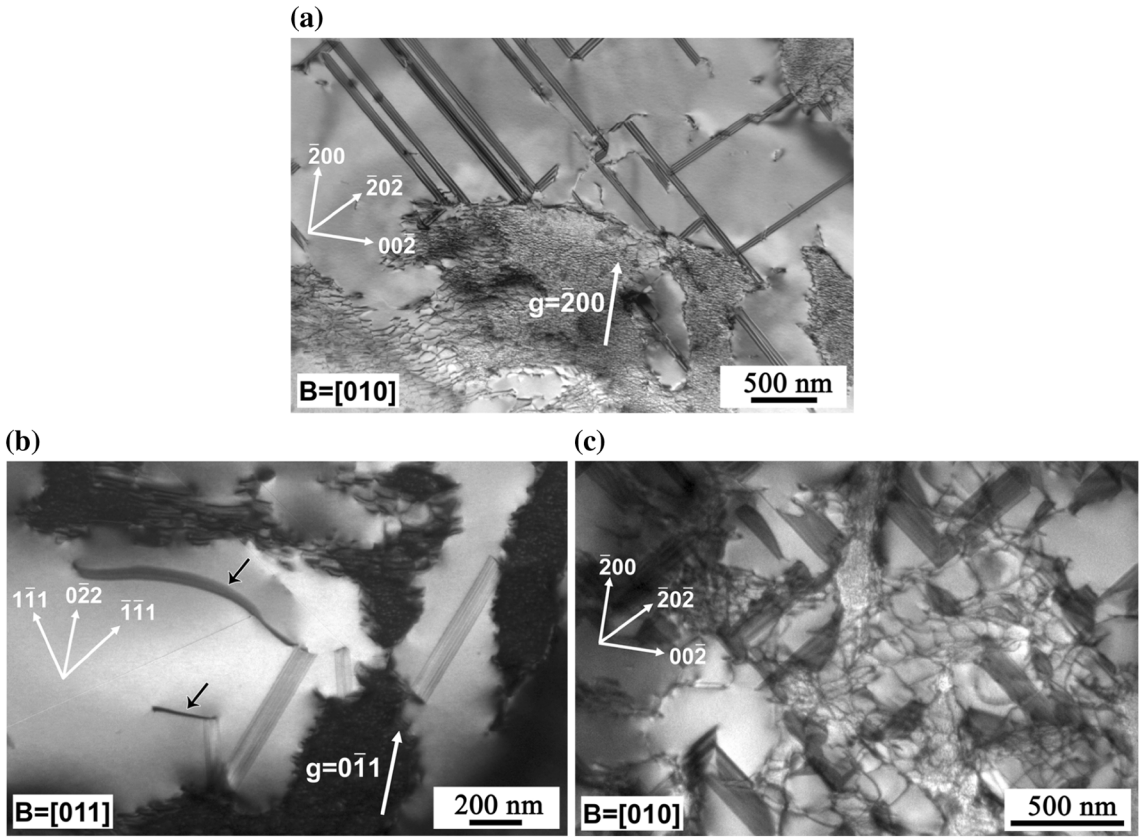

Fig. 7. Typical dislocation substructure of alloy TaTi after 1% creep strain: (a and b) 1000°C/137 MPa, B = [010] and g = $\bar{2}00$, B = [011] and g = $0\bar{1}1$; (c) 982°C/248 MPa, B = [010].

the γ single-phase region and changes to γ–γ'–χ three-phase and γ–γ' two-phase regions by respective Ta and Ti additions, indicating that Ti addition is more beneficial to the microstructural stability. With the combined additions and higher γ' solvus temperature, alloy TaTi appeared to reach γ–γ' two-phase equilibrium at 900°C, and it seemed unchanged at elevated temperature as the γ–γ' microstructure was stable after prolonged aging treatment at 1050°C. These trends suggest that the synergetic effects of Ta and Ti additions are more effective than the individual addition in promoting both the γ' thermal stability and microstructural stability above 1000°C. This also indicates that the

continued improvements of these microstructural features in these materials have been possible through the close control of alloy chemistry.

Creep Property and Deformation Mode

Figure 8 shows the Larson Miller parameter for Group I alloys and previous reported Co-Al-W-base and Ni-base single-crystal alloys. Under 900°C/420 MPa, quaternary Group I alloys exhibit higher creep strength than the ternary alloy, whereas quinary alloy has even better creep resistance. This is mainly because of the gradual increase of γ' volume fractions at 900°C resulting from higher γ' solvus temperatures with each additional component (Fig. 1 and Table I). As the γ' volume fraction increased, the number, density, and size of the γ' rafts increased, which has led to more dislocation motion resistance and lower creep rates in Ni-base single-crystal superalloys.[23] The rafts parallel to the applied stress are also expected to be beneficial to high-temperature mechanical properties such as fatigue resistance,[24] which is a promising feature for Co-base alloys. In alloy Ti and alloy TaTi, the phase stability without the formation of χ phase during creep at 900°C appears to be another reason for their superior creep resistance compared with alloy Ta (Fig. 5b).

The better creep resistance of alloy TaTi at 1000°C/137 MPa is related to the improved microstructural stability compared with Co-base alloy Co-9Al-10W-2Ta. Although the initial γ' volume fractions are similar, long-term aging at 1000°C of alloy TaTi revealed γ–γ' microstructure with 75.0% γ' volume fraction (Fig. 1b), whereas a similar exposure in Co-9Al-10W-2Ta alloy resulted in significant dissolution of γ' phase and appreciable secondary phase in volume fraction.[6] Under higher stress, the quinary alloy exceeded the multicomponent single-crystal superalloy CMSX-3 when crept at 982°C/248 MPa (Fig. 8), possibly because of the different deformation mechanism. In Ni-base single-crystal superalloys, the shearing of rafts by dislocation pairs coupled with APBs occurs at the beginning of the tertiary creep, when the rafting is complete and γ–γ' interfacial dislocation networks were developed.[23] In the current study after 1% creep strain (Fig. 7a and b), dislocations with SFs and APBs are frequently observed within γ' precipitates in addition to dislocation networks, suggesting that considerable cutting process by ⟨112⟩ slip has occurred. This deformation mode is partially consistent with the shearing mechanism under a high density of SFs observed in Co-9Al-8W-2Ta alloy after creep rupture at 1000°C,[6] suggesting that the SF energy in Co-Al-W-base alloys is lower than that in Ni-base alloys.[25] More work is required to clarify deformation mechanisms in γ'-strengthened Co-base alloys in relationship to changing SF energy and/or APB energy with the modification of alloy chemistry.

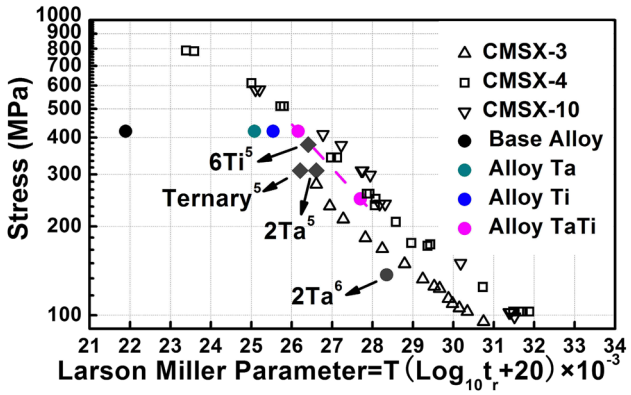

Fig. 8. Comparison of Larson Miller parameter of Group I alloys with previously reported Co-Al-W-base and Ni-base single-crystal alloys.[5,6]

SUMMARY

Single-crystal quinary Co-Al-W-Ta-Ti alloy shows higher γ' solvus temperature, improved microstructural stability, and higher γ' volume fraction at 900°C to 1050°C compared with quaternary alloys containing individual Ta and Ti additions, suggesting a synergetic effect. This alloy also possesses much better creep resistance at 900°C than the quaternary alloys with either Ta and Ti additions, and it exceeds both Co-base alloys and first-generation Ni-base single-crystal superalloys in creep life at around 1000°C. At these high γ' volume fractions, the superior creep resistance results from the formation of γ' rafts parallel to tensile stress axis, leading to deformation by γ–γ' interfacial dislocation networks as well as the shearing of γ' precipitates by ⟨112⟩ multiple slips with SFs and APBs. The current study clearly indicates that Co-Al-W-Ta-Ti-base alloys offer improved temperature capability and are expected to be potential candidates for further alloy development.

ACKNOWLEDGEMENTS

This work is financially supported by the National Natural Science Foundation of China (Nos. 50771012, 51201006, and 51301014), Aeronautical Science Foundation of China (No. 2009ZF74011), and New Century Excellent Talents in University (No. NCET-06-0079). The authors are very grateful to X.H. Li, Z.Q. Li, T. Mi, D.Z. Tang, Y.S. Zhao, Q.Y. Shi, M.L. Wang, X.F. Ding, and H. Chang for their contributions during the investigation of Co-base alloys in the past few years.

REFERENCES

1. R.C. Reed, *The Superalloys: Fundamentals and Applications* (Cambridge, U.K.: Cambridge University Press, 2006).
2. T.M. Pollock and S. Tin, *J. Propul. Power* 22, 361 (2006).
3. J. Sato, T. Omori, K. Oikawa, I. Ohnuma, R. Karinuma, and K. Ishida, *Science* 312, 90 (2006).
4. A. Suzuki and T.M. Pollock, *Acta Mater.* 56, 1288 (2008).
5. M.S. Titus, A. Suzuki, and T.M. Pollock, *Superalloys 2012*, eds. E.S. Huron, R.C. Reed, M.C. Hardy, M.J. Mills, R.E.

Montero, P.D. Portella, and J. Telesman (Warrendale, PA: The Minerals, Metals & Materials Society; Hoboken, NJ: John Wiley & Sons, 2012), pp. 823–832.
6. K. Tanaka, M. Ooshima, N. Tsuno, A. Sato, and H. Inui, *Philos. Mag.* 92 (2012), pp. 4011–4027.
7. T.M. Pollock, J. Dibbern, M. Tsunekane, J. Zhu, and A. Suzuki, *JOM* 62(1), 58 (2010).
8. T. Omori, K. Oikawa, J. Sato, I. Ohnuma, U.R. Kattner, R. Kainuma, and K. Ishida, *Intermetallics* 32, 274 (2013).
9. F. Xue, M. Wang, and Q. Feng, *Superalloys 2012*, eds. E.S. Huron, R.C. Reed, M.C. Hardy, M.J. Mills, R.E. Montero, P.D. Portella, and J. Telesman (Warrendale, PA: The Minerals, Metals & Materials Society; Hoboken, NJ: John Wiley & Sons, 2012), pp. 813–821.
10. A. Bauer, S. Neumeier, F. Pyczak, R.F. Singer, and M. Göken, *Mater. Sci. Eng. A* 550, 333 (2012).
11. F. Xue, Z.Q. Li, and Q. Feng, *Mater. Sci. Forum* 654–656, 420 (2010).
12. F. Xue, M.L. Wang, and Q. Feng, *Mater. Sci. Forum* 686, 388 (2011).
13. A. Bauer, S. Neumeier, F. Pyczak, and M. Göken, *Superalloys 2012*, eds. E.S. Huron, R.C. Reed, M.C. Hardy, M.J. Mills, R.E. Montero, P.D. Portella, and J. Telesman (Warrendale, PA: The Minerals, Metals & Materials Society; Hoboken, NJ: John Wiley & Sons, 2012), pp. 695–703.
14. M.S. Titus, A. Suzuki, and T.M. Pollock, *Scripta Mater.* 66, 574 (2012).
15. F. Xue, H.J. Zhou, X.H. Chen, Q.Y. Shi, H. Chang, M.L. Wang, X.F. Ding, and Q. Feng, *Eurosuperalloys 2014*, eds. J.Y. Guédou and J. Choné (Les Ulis, France: EDP Sciences, 2014), 15002.
16. F. Xue, H.J. Zhou, X.F. Ding, M.L. Wang, and Q. Feng, *Mater. Lett.* 112, 215 (2013).
17. X.H. Li, B. Gan, Q. Feng, Z.Q. Sun, G.L. Chen, G.Q. Zhang, and L.M. Cao, *J. Univ. Sci. Technol. Beijing* 30, 1369 (2008).
18. F. Xue, T. Mi, M.L. Wang, X.F. Ding, X.H. Li, and Q. Feng, *Acta Metall. Sin.* 50, 845 (2014).
19. G.L. Erickson and K. Harris, U.S. patent 4643782 (1987).
20. M. Condat and B. Décamps, *Scripta Metall.* 21, 607 (1987).
21. S. Kobayashi, Y. Tsukamoto, and T. Takasugi, *Intermetallics* 31, 94 (2012).
22. S. Kobayashi, Y. Tsukamoto, and T. Takasugi, *Intermetallics* 19, 1908 (2011).
23. T.M. Pollock and R.D. Field, *Dislocations in Solids*, Vol. 11, eds. F.R.N. Nabarro and M.S. Duesbery (Amsterdam, The Netherlands: Elsevier, 2002), pp. 547–618.
24. H. Mughrabi, M. Ott, and U. Tetzlaff, *Mater. Sci. Eng. A* 234–236, 434 (1997).
25. P.C.J. Gallagher, *Metall. Trans.* 1, 2429 (1970).